

Table 2. Proportions of organelles in subcellular fractions of fresh liver of Lake Michigan lake trout

Organelle	Nuclear	Mitochondrial Heavy	Light	Microsomal ^a	Soluble
Nucleus	0.271				
Mitochondria	0.019	0.422	0.652	0.022	
Lipid droplets	0.052	0.075	0.078	0.007	0.003
Membranes	0.027				
Rough endoplasmic reticulum		0.087	0.083	0.335	
Ribosomes				0.171	
Cytoplasmic debris	0.088				0.008
Particulate cytoplasmic debris		0.148	0.169		
Non-specific cytoplasmic debris				0.024	
Submicroscopic material	0.543	0.269	0.018	0.441	0.989

^aThe proportions of organelles in the microsomal fraction were calculated on an area basis since the few mitochondria present were swollen and their volume was disproportionately large.

Table 3. Calculated proportion of mercury by volume in subcellular organelles of fresh liver of Lake Michigan lake trout

Organelle	Proportion of mercury (p ± SE)
Nuclei	0.025 ± 0.0012
Mitochondria	0.055 ± 0.0012
Lipid droplets	0.015 ± 0.0014
Membranes	0.002 ± 0.0004
Rough endoplasmic reticulum	0.050 ± 0.0018
Ribosomes	0.021 ± 0.0014
Cytoplasmic debris	0.014 ± 0.0019
Particulate cytoplasmic debris	0.015 ± 0.0007
Nonspecific cytoplasmic debris	0.003 ± 0.0006
Submicroscopic material	0.799 ± 0.0031

fractions and made up 50–80% of the total tissue mercury. They identified a metallothionein-like protein in the liver cytosol that bound about 40% of the mercury. Marafante³ also reported the presence of a cytosol protein that bound mercury in liver of goldfish (*Carassius auratus*). These metallothionein-like proteins, first discovered in horse kidney by Margoshes and Vallee¹², serve as a protective mechanism for animals¹³. Hence, we suggest that lake trout are partly protected from the toxic effects of mercury by the binding of the metal to a metallothionein-like protein in the submicroscopic material of the liver.

- 1 Contribution 582 of the Great Lakes Fishery Laboratory, U.S. Fish and Wildlife Service, Ann Arbor, Michigan 48105. We thank Dr T.F. Beals (Veterans Administration Medical Center, Ann Arbor) for helpful discussions of electron micrographs, P.M. Haack for statistical analysis, and W.A. Willford for critical review of the manuscript.
- 2 Present address: Department of Biochemistry, University of Chicago, 920 East 58th Street, Chicago (Illinois 60637, USA).
- 3 E. Marafante, *Experientia* 32, 149 (1976).
- 4 K.R. Olson, K.S. Squibb and R.J. Cousins, *J. Fish. Res. Bd Can.* 35, 381 (1978).
- 5 Michigan Department of Agriculture, Great Lakes environmental contaminants survey 1975. Mich. Dept. Agric., Lansing, Michigan 1975.
- 6 G.H. Hogeboom, in: *Methods in enzymology*, vol. 1, p. 16. Eds S.P. Colowick and N.O. Kaplan. Academic Press, New York 1955.
- 7 S. Fleischer and M. Kervina, in: *Methods in enzymology*, vol. 31, part A, p. 6. Eds S. Fleischer and L. Packer. Academic Press, New York 1974.
- 8 C.J. Dawes, *Biological techniques in electron microscopy*. Barnes and Noble, New York 1971.
- 9 E.R. Weibel, in: *International review of cytology*, vol. 26, p. 235. Eds G.H. Bourne and J.F. Danielli. Academic Press, New York 1969.
- 10 W.A. Willford, R.J. Hesselberg and H.L. Bergman, *J. Ass. off. analyt. Chem.* 56, 1008 (1973).
- 11 W.G. Cochran, *Sampling techniques*, 3rd edn, p. 52. Wiley, New York 1977.
- 12 M. Margoshes and B.L. Vallee, *J. Am. chem. Soc.* 79, 4813 (1957).
- 13 F. Noel-Lambot, *Experientia* 32, 324 (1976).

Rat sternothyroid muscle: Dissection and preparation for electrophysiologic and electronmicrographic studies¹

D.H. Lambert^{2,3} and D.A. Barone⁴

Department of Neurology, University of Vermont College of Medicine, Burlington (Vermont 05401, USA), 26 October 1981

Summary. The sternothyroid muscle of the rat is described. The ease of dissection and localization of end-plate regions within the sternothyroid muscle by direct visualization of nerve supply provides a convenient mammalian muscle preparation for electrophysiological and ultrastructural research.

In a recent publication, Dreyer et al.⁵ characterized the omohyoideus muscle of the mouse as a convenient mammalian muscle preparation for use with Nomarski interference optics in electrophysiological investigations of the neuromuscular junction. Because of its insertion onto the scapula, we have found dissection of the omohyoideus muscle cumbersome. As a result, an alternative preparation, the rat sternothyroid muscle, has been evaluated.

Materials and methods. More than 50 female Lewis rats weighing 150–220 g were studied. The dissection consisted of reflecting the sternal heads of the sternomastoid muscles from the sternum, thereby freeing the sternohyoid muscles from the sternum; dissecting the sternohyoid muscles free of each other in the midline; bisecting the trachea transversely; splitting the larynx and proximal trachea in the midline; and finally dissecting the sternohyoid muscle free

of the hyoid bone and underlying soft tissues. We found that the sternothyroid muscle originates from a tendinous origin in the proximal portion of the sternohyoid muscle, and the dissection, as described, results in a block of tissue comprised of the sternohyoid muscle, the sternothyroid muscle and one-half of the thyroid cartilage, cricoid cartilage and superior trachea. By grasping the thyroid cartilage with fine forceps, the sternothyroid muscle may then be easily teased from the overlying sternohyoid muscle. The nervous innervation of the sternothyroid muscle, the ansa

hypoglossus, is readily dissected with the muscle when required. The bathing media⁶ and the optics used to visualize the preparation⁷ have been described previously. The bathing solution was not oxygenated and the temperature ranged between 20 and 23 °C. The electrophysiologic recordings and the preparation of tissue for lightmicroscopy and electronmicroscopy were accomplished using conventional methods.

Results. Figure 1A shows the sternothyroid muscle (ST) attached to the thyroid cartilage (TC) and the sternohyoid muscle (SH). The nerve innervating the sternothyroid muscle, the ansa hypoglossus (AH), enters the muscle at approximately one-third the distance from origin to insertion (arrow) and traverses diagonally to the upper one-third of the muscle.

Figure 1B demonstrates how the end-plates are distributed along the course of the nerve. The pattern of innervation was remarkably constant from muscle to muscle and animal to animal. This constancy and pattern of innervation facilitates the localization of end-plates for ultrastructural studies. After fixing the muscle, it is necessary only to cut along each side of the easily visualized nerve to obtain tissue rich in end-plates (EP). In the fresh preparation, locating areas where myelin twigs (MT) depart from the nerve pinpoints end-plates for electrophysiological recording. Although no attempt was made to statistically assess

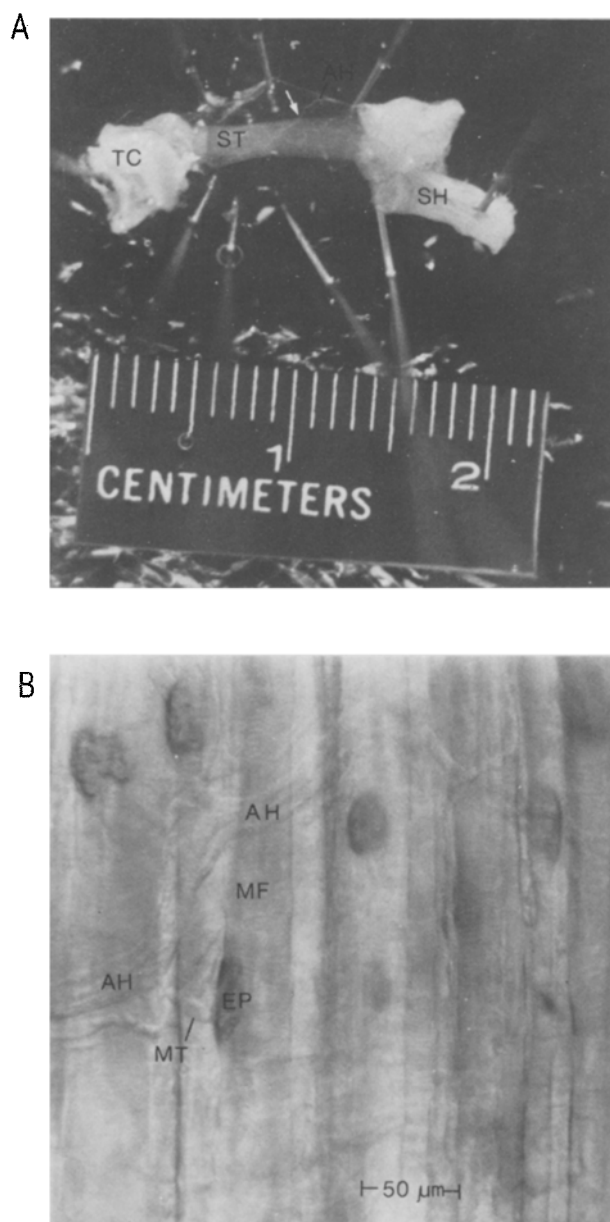


Figure 1. *A* Photomicrograph of the sternothyroid muscle (ST) showing its attachment to the thyroid cartilage (TC) and to the sternohyoid muscle (SH). The muscle is innervated by the ansa hypoglossus (AH). The arrow indicates the point of entry of the ansa hypoglossus into the muscle. *B* Photomicrograph showing the distribution of end-plates along the course of the ansa hypoglossus (AH). Myelin twigs (MT) leave the nerve and eventually synapse with the muscle fibers (MF) forming an end-plate (EP). The end-plates have been stained for acetylcholinesterase.

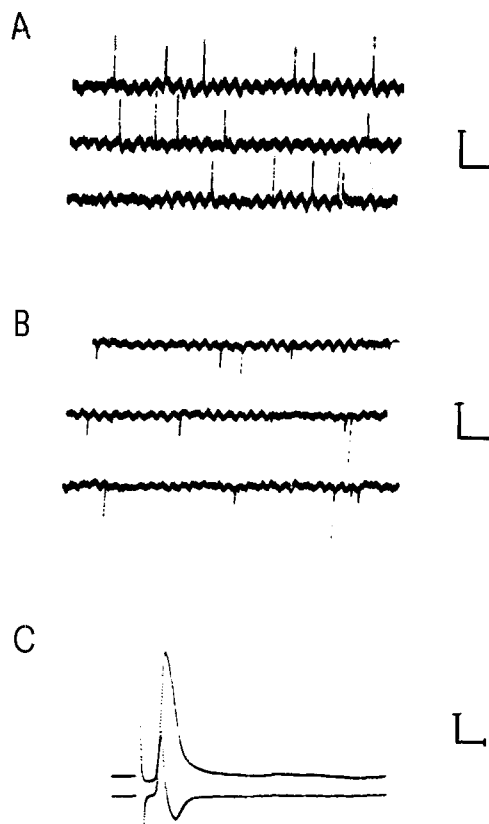


Figure 2. Examples of recordings made from the sternothyroid muscle with microelectrodes. *A* and *B* Miniature end-plate potentials recorded intracellularly and extracellularly, respectively. *C* Muscle action potential recorded intracellularly following indirect stimulation. The resting potential was -70 mV in this cell. The overshoot was +20 mV. The lower trace represents dVm/dt, obtained by electronic differentiation. Calibrations: *A*) 0.5 mV vertically, 50 msec horizontally. *B*) 1 mV vertically, 50 msec horizontally. *C*) 20 mV vertically, 1 msec horizontally for the action potential and 200 V/sec vertically, 1 msec horizontally for dVm/dt.

mean fiber diameter, the muscle fibers were in the 30–45 μm range (see fig. 1B).

Figure 2 is a composite of examples of electrophysiologic recordings made from the sternothyroid muscle. Under the conditions described in the methods section, resting potentials between -65 and -78 mV were readily obtained. Figure 2A and B are examples of miniature end-plate potentials (MEPPs) recorded intracellularly and extracellularly, respectively. The mean MEPP amplitude (corrected to a resting potential of -90 mV) recorded intracellularly was 0.71 mV. Figure 2C shows an intracellularly recorded action potential resulting from indirect stimulation via the ansa hypoglossus nerve.

Discussion. Because the rat sternothyroid muscle is considerably thicker than the mouse omohyoid muscle, it is probably unsuitable for use with Normarski optics, except at the lateral edges where it is only a few fibers thick. Nevertheless, the ease of localizing end-plates within the rat sternothyroid muscle, as described, is a great advantage. Localization of end-plate regions for electronmicroscopic evaluation has always presented a problem. Engel's method⁸ for locating end-plates consists of cutting fixed muscle into 2 strips; reacting one strip with acetylcholinesterase stain; embedding the reacted and unreacted strips parallel to each other; viewing both strips in the dissection microscope; and removing and reembedding the region in the unreacted muscle strip which corresponds to the stained end-plate region in the reacted strip. Since the 'motor point' (zone where end-plates are concentrated) in the sternothyroid muscle is located adjacent to the readily visualized

nerve which innervates it, the sternothyroid 'motor point' is readily excised by cutting along each side of the nerve. This technique has provided us with ample end-plates for electronmicroscopic evaluation⁹ without having to employ the more cumbersome and time-consuming method described by Engel⁸. With practice, the dissection can be accomplished in 5–10 min. This coupled with the ability to visualize the end-plate region and visually control impalements also makes the preparation very suitable for electrophysiological studies.

- 1 This research was supported in part by the following grants: PHS 5429-16-20 (to C.M. Poser), NIH grant NS-07740 (to R.L. Parsons).
- 2 We express our appreciation to Drs C.M. Poser and R.L. Parsons for providing us with laboratory space and equipment to conduct these experiments in addition to much helpful advice and criticism.
- 3 Present address: Department of Anesthesia, Brigham and Women's Hospital, 75 Francis Street, Boston (Massachusetts 02115, USA).
- 4 Present address: Neurology Section, Department of Medicine, College of Medicine and Dentistry of New Jersey, New Jersey School of Osteopathic Medicine, 300 Broadway, Camden (New Jersey 08103, USA).
- 5 F. Dreyer, K.-D. Müller, K. Peper and R. Sterz, *Pflügers Arch.* 367, 115 (1976).
- 6 A. W. Liley, *J. Physiol.* 132, 650 (1956).
- 7 D.H. Lambert and R.L. Parsons, *J. gen. Physiol.* 56, 309 (1970).
- 8 A.G. Engel, *Mayo clin. Proc.* 45, 450 (1970).
- 9 D.A. Barone, D.H. Lambert and C.M. Poser, *Archs Neurol.* 37, 663 (1980).

Leydig cell and Δ^5 - 3β -hydroxysteroid dehydrogenase activity in the testis of toad (*Bufo melanostictus*) following cold exposure

P. B. Patra and N. M. Biswas

Histology and Histochemistry Laboratory, Department of Physiology, University Colleges of Science and Technology, 92, Acharya Prafulla Chandra Road, Calcutta 700 009 (India), 6 October 1980

Summary. Leydig cell nuclear area and Δ^5 - 3β -hydroxysteroid dehydrogenase activity were increased in the testis of *Bufo melanostictus* 2 days after a single short-term cold exposure. Both parameters returned to normal values 4 days later.

The influence of ambient temperature on testicular activity in different classes of vertebrates is well established¹⁻⁴. Compared with heat, cold is much less severe in its effect on testicular function of mammals and much greater extremes are required to produce an effect in higher vertebrates^{5,6}. However, little is known about the influence of severe hypothermia on the amphibian testis. In view of the above findings the present study was undertaken to elucidate whether severe cold exposure can alter the testicular endocrine activity in amphibia. Testicular steroidogenic activity in *Bufo melanostictus* was evaluated mainly by demonstrating histochemically Δ^5 - 3β -hydroxysteroid dehydrogenase (Δ^5 - 3β -HSD), a key enzyme of steroid hormone production in both mammalian and non-mammalian vertebrates⁷⁻⁸.

Materials and methods. 70 male toads of average body weight 56 g were used in the present experiment. All the animals were collected from their natural habitat during the breeding season (June/July). They were kept in the laboratory for a few days prior to experimentation in the presence of water and normal periods of light and darkness. Ant eggs were supplied as food on alternate days.

40 toads were exposed to cold in a cold chamber at -2°C for 3 h. At the end of the exposure they were taken out of the chamber for revival. 75% of the exposed toads revived. The animals were divided equally into 3 groups. Group A: unexposed control animals; group B: exposed toads sacrificed 2 days after cold exposure; group C: exposed toads sacrificed 6 days after cold exposure; group D: exposed toads sacrificed 10 days after cold exposure.

The animals were sacrificed according to their scheduled date of sacrifice along with controls. Fresh frozen sections from 1 testis were cut at $20\ \mu\text{m}$ on a cryostat at -20°C for histochemical demonstration of Δ^5 - 3β -hydroxysteroid dehydrogenase (Δ^5 - 3β -HSD) using dehydroepiandrosterone as substrate⁹. Control sections were incubated simultaneously for the same time period in a medium containing no substrate. After incubation, sections were fixed in 10% formol, washed in distilled water, dried and mounted in glycerine jelly. Another testis was fixed in Bouin's fluid for histometric studies of Leydig cell nuclear area (LCNA) according to Deb et al.¹⁰. For histology, $5\text{-}\mu\text{m}$ sections were prepared and stained with hematoxylin-eosin.

Results and discussion. Δ^5 - 3β -HSD activity was localized